Portugaliae Electrochimica Acta 2011, 29(5), 335-342

DOI: 10.4152/pea.201105335

PORTUGALIAE ELECTROCHIMICA ACTA
ISSN 1647-1571

Improving Electrocatalytic Activity of $LaNiO_3$ Films by Deposition on Foam Nickel Substrates

C.O. Soares,[1] M.D. Carvalho,[1] M.E. Melo Jorge,[1] A. Gomes,[1] R.A. Silva,[2] C.M. Rangel,[2] M.I. da Silva Pereira[1,*]

[1] *C.C.M.M., Departamento de Química e Bioquímica da Faculdade de Ciências da Universidade de Lisboa, Campo Grande, 1749-016 Lisboa, Portugal*
[2] *Laboratório Nacional de Energia e Geologia, Paço do Lumiar 22, Fuel Cells and Hydrogen Unit, 1649-038 Lisboa, Portugal*

Received 28 December 2010; accepted 23 February 2011

Abstract

In this work $LaNiO_3$ oxide was prepared by a self-combustion method using citric acid. The electrodes were obtained by coating a nickel foam support with the oxide suspension. Optical microscopy and cyclic voltammetry were used on the electrodes characterization. The evaluation of the electrodes electrocatalytic activity, towards the oxygen evolution reaction in alkaline medium, was performed by means of steady state measurements.

The reaction follows a first order kinetics, with respect to OH^- concentration, with Tafel slopes close to 40 mV, for low overpotentials. Based on the apparent and real current densities it was possible to conclude that the increase on the electrode activity, when compared with the published data, is mostly related to geometric factors. This fact has been associated with the high electrode/electrolyte contact area provided by the foam nickel substrate. Synergetic effects between the Ni foam and the perovskite oxide cannot be discarded.

Keywords: $LaNiO_3$ electrode, nickel foam, oxygen evolution, electrocatalysis.

Introduction

Search for new or improved electrode materials is restless in the field of power sources, namely, of batteries and fuel cells. One of the challenging problems in the area is to find an effective electrode material that operates alternatively as anode and cathode and catalyses the oxygen electrochemical reactions (bifunctional oxygen electrode) [1, 2]. Perovskite type oxide materials are

* Corresponding author. E-mail address: mipereira@fc.ul.pt

considered potential candidates since they can catalyse oxygen evolution and reduction, simultaneously. Several studies found in the literature suggest that Ni containing perovskites are among the most active [3-10]. Indeed $LaNiO_3$ is one of the best catalysts for the oxygen evolution reaction (OER), in alkaline medium, and it is also reported as a good catalyst for the oxygen reduction reaction (ORR) [11].

It is well known that the properties and behaviour of the $LaNiO_3$ electrode depend on the oxide preparation method, the experimental conditions, and in particular the support employed in the electrode construction [7,11,12]. Consequently, the kinetic parameters for oxygen evolution and reduction might vary.

The main goal of the work presented in this paper is the development of stable $LaNiO_3$ electrodes, with enhanced electrocatalytic activity towards the OER, using as support Ni foam.

To our knowledge this is the first report of construction of a $LaNiO_3$ electrode using Ni foam as support.

Experimental

The perovskite-type oxide $LaNiO_3$ was prepared by a self-combustion method using citric acid. Stoichiometric amounts of La_2O_3 (99.95%, Sigma Aldrich), previously heated at 1173 K and Ni (99.99%, Sigma Aldrich) were separately dissolved in HNO_3 (69%, Sigma Aldrich). Citric acid (99%, Sigma Aldrich) was added, in equal amount, to the total metal ions. The solution was heated up, on a sand bath, with consequent degradation and combustion of the resulting gel. The dry product obtained was heated at 873 K for 6 h in order to remove the reminiscent organic matter, and the resulting powder was finally heated at 1173 K in air for 12 h.

The formation of the perovskite-type phase was confirmed by X-ray diffraction (XRD) using a Philips PW 1730 X-ray powder diffractometer, operating with Cu $K\alpha$ radiation.

The films were prepared by coating (brush painting) nickel foam supports (Goodfellows), typically 1 cm × 1 cm, with a suspension of the oxide on TritonX-100 Fluke Chemie AG. After each application, the solvent was evaporated and the dried layer fired, in an oven, till the temperature reaches 673 K (≈ 4 h) followed by 3 h at 673 K. The oxide loading was around 89±5 mg cm^{-2}. The samples were then mounted in a glass tube with Araldite epoxy resin, so that the electrolyte could only make contact with the oxide. Three specimens were prepared two for electrochemical experiments and one for morphological characterization.

The global aspect of the electrodes was observed by optical microscopy (Nikon SMZ 1500).

A conventional three-electrode glass cell was used. The measurements were carried out at room temperature, using Hg/HgO (+0.098V vs. SHE) and Ni foam as reference and counter electrodes, respectively. A Voltalab 10 (PGZ100)

Radiometer apparatus controlled by a personal computer through the VoltaMaster 4 software has been used.
The potassium hydroxide 1 M solution (>90%, Sigma Aldrich) was prepared using Millipore Milli-Q ultrapure water (18 MΩ). Prior to each electrochemical measurement, the KOH 1 M solution was purged with high-purity N_2.
Steady state measurements were performed after stabilising the electrode at 0.720 V vs. Hg/HgO, for 10 min, in order to obtain a stable surface, prior to the measurements. Measurements were recorded from the higher to the lower potential value.

Results and discussion

Optical microscopy

The morphology of the $LaNiO_3$ coating was examined by optical microscopy, before and after being used as anode for the OER, in order to confirm that the Ni foam substrate was suitably covered with the oxide. For comparison, the images of the Ni foam were recorded. Fig. 1 shows the representative global aspect of the new (a), used (b) electrodes and the uncovered Ni foam support (c). The porosity of the nickel foam is evident from the image. Concerning the $LaNiO_3$ coating, the Ni foam support is almost fully covered by the oxide, although some uncovered Ni points are observed. The coating is characterized by an irregular surface, indicating high roughness. The electrode images, after and before being used for oxygen evolution, do not show significant variations.

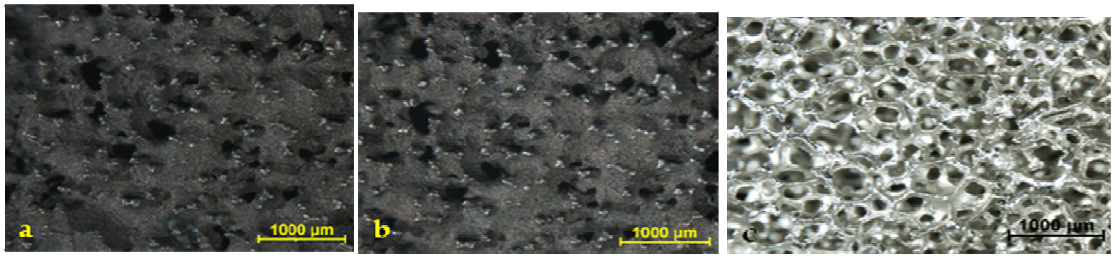

Figure 1. Optical microscope images of the Ni/$LaNiO_3$ electrode, (a) before and (b) after being used for oxygen evolution. Ni foam (c). (30 ×)

Cyclic voltammetry

Fig. 2 shows a representative stabilized cyclic voltammogram recorded for a Ni/$LaNiO_3$ coated electrode in 1 M KOH at a sweep rate of 10 mV s^{-1}. For all the electrodes, an anodic and the corresponding cathodic peak are observed, prior oxygen evolution, usually assigned to the redox pair Ni^{3+}/Ni^{2+}[7-10]. The estimated formal redox potential associated with this pair of peaks is within the range of those published, for the same oxide electrodes [7, 8]. In the negative potential range a cathodic peak is observed around -0.170 V vs. Hg/HgO attributed to the oxygen reduction [10]. The cyclic voltammograms run after and before the oxygen evolution showed similar features.

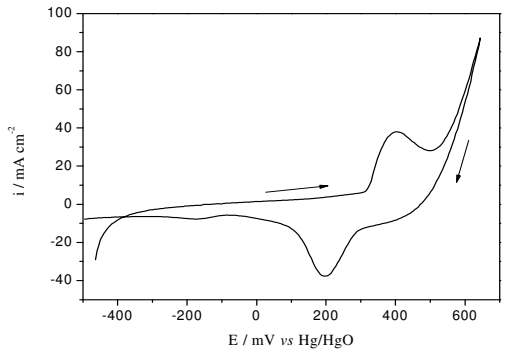

Figure 2. Cyclic voltammogram for $Ni/LaNiO_3$ electrode in 1 M KOH solution at a scan rate of 10 mV s^{-1}.

Oxygen evolution reaction

The study of the electrocatalytic activity of the prepared electrodes, towards the oxygen evolution reaction was studied in 1 M KOH solutions in the potential range of 0.500 - 0.720 V vs. Hg/HgO. Fig. 3 shows a representative Tafel plot, without Ohmic drop correction, for a freshly prepared $Ni/LaNiO_3$ coated electrode. As Fig, 3 shows, meaningful current intensities could be measured for potentials higher than 0.500 V vs. Hg/HgO. Once the standard potential of the oxygen electrode in basic solution is +0.300 V vs. Hg/HgO, it can be said that a minimum overpotential of ≈ 0.200 V is needed for oxygen evolution to occur.

Linear plots for *log i* vs. *E* were obtained over less than 1 decade of current, in the potential range of 0.520-0.580 V (see Fig. 3 inset). Deviations at more anodic potentials can be due either to uncompensated Ohmic drops or to a second Tafel line + IR drops. The calculated Tafel slope has the value of 56 ± 4 mV. Values between 40 and 60 mV can be found in the literature, for this potential region, depending on the oxide preparation method, oxide support and electrode type [4, 7, 9, 13].

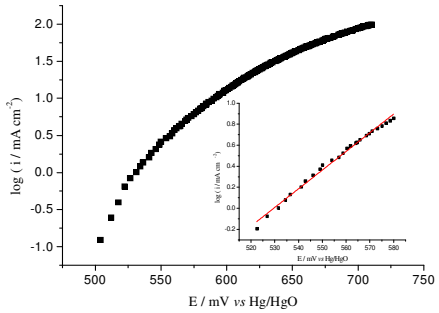

Figure 3. Tafel plot for oxygen evolution on $Ni/LaNiO_3$ electrode in 1 M KOH solution without Ohmic drop correction. Inset: linear region of the Tafel plot.

The most striking feature on the log *i* vs. *E* plots is the extremely narrow Tafel region. Similar behaviour has been observed by some of us for spinel type Fe - Co_3O_4 thin film [14] and Li-Co_3O_4 electrodes [15]. A detailed analysis of the data led us to conclude that the observed deviations, from Tafel behaviour, were a

result of uncompensated Ohmic drops due to the electrode and electrolyte resistances as well as oxygen bubbles surface obstruction.
In order to distinguish between Ohmic drops or a second Tafel line, the Ohmic drops were estimated, following the methodology proposed by Boodts and Trasatti [16].

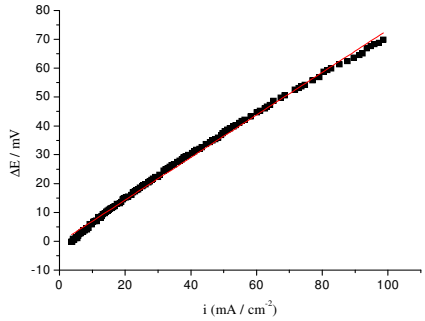

Figure 4. Plot of ΔE *vs.* i for the curve presented in Fig. 3.

Fig. 4 shows the relationship of the potential difference ΔE, measured at constant current, between the experimental points and the extended Tafel line and the current density, in the potential range 0.560 – 0.710 V vs. Hg/HgO. The linearity indicates that the deviations from the Tafel behaviour are only due to uncompensated Ohmic drops and that only one Tafel line exists in this potential region. From the slope a value of 0.74±0.1 Ω cm^{-2} was evaluated for the uncompensated resistance between the electrode surface and the tip of the Luggin capillary, as well as the resistance of the oxide overlayer.

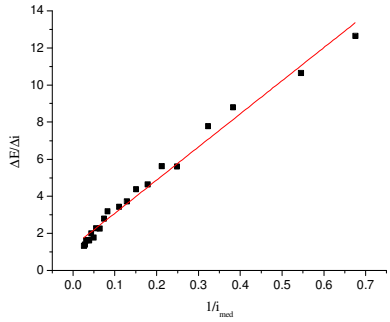

Figure 5. Plot of $\Delta E/\Delta i$ *vs.* $1/i$ for the curve presented in Fig. 3.

As in the presence of uncompensated Ohmic drops Tafel equation can be written as $E=a + b\ lni + iR$, it results $dE/di=b/i + R$ [14, 17]. Fig. 5 shows the plot of $\Delta E/\Delta i$ *vs.* $1/i$, being ΔE and Δi the difference of two consecutive experimental points and i the mean value between two consecutive values. A single straight line is observed whose slope ×2.303 gives b and whose intercept gives R. Considering that a correlation factor of 0.9840 has been achieved, it can be concluded that the deviations on the Tafel slope, in the potential region from 0.540 V to 0.650 V, are due to uncompensated Ohmic drops and oxygen bubbles surface obstruction. Moreover the OER mechanism does not change within this potential range.

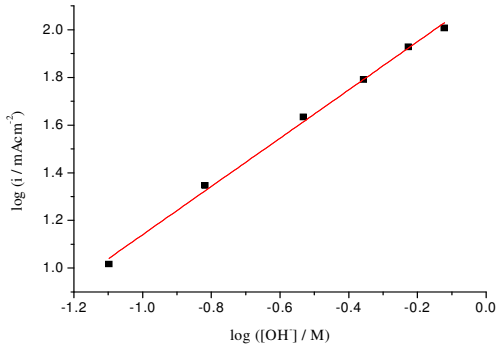

Figure 6. Plot of log *i vs.* log [OH^-] for Ni/$LaNiO_3$ electrode in 1 M KOH solution at E=0.683 V *vs.* Hg/HgO.

From the slope of the plot of $\Delta E/\Delta i$ *vs.* $1/i$ the corrected Tafel slope has been calculated and a value of 45±3 mV was obtained. This value is similar to the lowest values found in the literature for $LaNiO_3$ oxide electrodes, in the forms of pellets [4] and thin films on platinum [7], at low potentials.
The reaction order with respect to OH^- was obtained from E vs. log i curves recorded at varying concentrations of KOH at constant ionic strengths, using KNO_3 as the inert electrolyte. An order of 1.0 was estimated from the slope of the plot, *log i vs. log* [OH^-] at 683 mV vs. Hg/HgO (Fig. 6). The reaction order and the Tafel slope observed indicate a mechanism similar to that already given by Bockris and Otagawa [18].

Table 1. Electrode kinetic parameters for oxygen evolution on Ni/$LaNiO_3$ electrodes in 1 M KOH.

Electrode	Oxide preparation method	Tafel slope/mV	R_f	$i_{0a} \times 10^9$/ A cm^{-2}	$i_{0t} \times 10^{12}$/ A cm^{-2}	Reaction order	Reference
Ni / $LaNiO_3$	Self-combustion	45	3528*	9.89	2.80	1.0	This work
Pt / $LaNiO_3$	Spray pyrolysis	45	170	0.07	0.412	2.2	[7]
$LaNiO_3$ (pellet)	Coprecipitation	43	5600	6.30	1.13	0.95	[4]

* Reference [19]; i_{0a} exchange current density based on geometrical surface area; i_{0t} exchange current density based on true surface area

To get a better insight on the OER kinetics, the apparent exchange current density (i_{0a}) has been evaluated. In order to eliminate geometric effects and discriminate the geometric and electronic effects, the value of the true exchange current density i_{0t} (= i_{0a}/R_f), has been calculated by normalising i_{0a} to unit real surface area, taking into account the oxide roughness factor (R_f) [19], estimated from voltammetric curves, recorded in a narrow range of potential, near the open circuit potential [20].
Table 1 presents the estimated kinetic parameters for the OER on Ni/ $LaNiO_3$ electrodes. For the purpose of comparison, data for $LaNiO_3$ electrodes prepared by different methods, and presenting Tafel slopes of the same order, are shown.

This table shows that among all the $LaNiO_3$ electrodes, the ones prepared in this work present the highest apparent exchange current density, what can be ascribed to the high roughness factor. Considering that the steady state measurements, for all the electrodes, gave similar Tafel slopes, the highest value for the true exchange current density, for the coatings on Ni foam, indicates that electronic effects are operating besides geometric effects, probably a contribution from the Ni foam support.

The enhanced activity, towards the oxygen evolution reaction, of the electrodes prepared in this work, has been confirmed by the comparison between the potential values measured at 100 mA cm^{-2} of apparent current density for $LaNiO_3$ films prepared by thermal decomposition and sequential coating, on Ni plates, under varying conditions [8]. A value of 0.760 V *vs.* Hg/HgO is reported for the most active electrode, while a lower value of 0.715 V *vs.* Hg/HgO was obtained in this work. Similarly higher values, 0.728 V *vs.* Hg/HgO, are quoted for $LaNiO_3$ films prepared by oxide-slurry painting, from powders prepared by the hydroxide solution precursor method [9].

Conclusions

In our exploration of new supports for the $LaNiO_3$ oxide we have successfully made use of Ni foam. It was found that the oxide preparation procedure by the self-combustion method, using citric acid, in combination with the use of Ni foam as support, enhanced the electrode surface properties. Consequently its electrocatalytic activity, towards the OER, is higher when compared with the reported in the literature for the same oxide electrode prepared by other methods. The better performance exhibited is due to the electrochemical properties of foam–oxide films originated from their highly porous morphologies. Synergetic effects between the Ni foam and the perovskite oxide cannot be discarded.

Acknowledgements

This work is partially financed by Fundação para a Ciência e Tecnologia (FCT), under contract nº PTDC/CTM/102545/2008. C.O. Soares acknowledges a grant from FCT under the same contract.

References

1. L. Jorissen, *J. Power Sources* 155 (2006) 23-32.
2. M. Bursell, M. Pirjamali, Y. Kiros, *Electrochim. Acta* 47 (2002) 1651-1660.
3. K. Kinoshita, *Electrochemical Oxygen Technology, The Electrochemical Society series, Wiley, New York,* 1992.
4. T. Otagawa, J. O'M. Bockris, *J. Electrochem. Soc.* 131 (1984) 290-302.
5. J. O'M. Bockris, T. Otagawa, V. Young, *J. Electroanal. Chem.* 150 (1983) 633-643.
6. J. O'M. Bockris, T. Otagawa, *J. Electrochem. Soc.* 129 (1982) 2391-2392.

7. R.N. Singh, L. Bahadur, J.P. Pandey, S.P. Singh, P. Chartier, G. Poillerat, *J. Appl. Electrochem.* 24 (1994) 149-156.
8. S.P. Singh, R.N. Singh, G. Poillerat, P. Chartier*, Int. J. Hydrogen Energy* 20 (1995) 203-210.
9. R.N. Singh, A.N. Jain, S.K. Tiwari, G. Poillerat, P. Chartier*, J. Appl. Electrochem.* 25 (1995) 1133-1138.
10. R.N. Singh, S.K. Tiwari, S.P. Singh, A.N. Jain, N.K. Singh*, Int. J. Hydrogen Energy* 22 (1997) 557-562.
11. S.K. Tiwari, J.F. Koenig, G. Poillerat, P. Chartier, R.N. Singh, *J. Appl. Electrochem.* 28 (1998) 114–119.
12. S. Trasatti, *in Electrochemistry of Novel Materials,* J. Lipkowski, P.N. Ross, Eds, VCH, New York, 1994.
13. R.N. Singh, S.K. Tiwari, T. Sharma, P. Chartier, J.F. Koenig, *J. New Mat. Electrochem. Sys.* 2 (1999) 65-69.
14. E. Laouini, M. Hamdani, M.I.S. Pereira, J. Douch, M.H. Mendonça, Y. Berghout, R.N. Singh, *Int. J. Hydrogen Energy* 33 (2008) 4936-4944.
15. M. Hamdani, M.I.S. Pereira, J. Douch, Y. Berghout, M. H. Mendonça*, Electrochim. Acta* 49 (2004) 1555-1563.
16. J.C.F. Boodts, S. Trasatti, *J. Appl. Electrochem.* 19 (1989) 255-262.
17. L. Popa, E. Guerrini, S. Trasatti, *J. Appl. Electrochem.* 35 (2005) 1213-1223.
18. J. O'M. Bockris, T. Otagawa*, J. Phys. Chem.* 87 (1983) 2960-2971.
19. C.M. Rangel, C.O. Soares, R.A. Silva, M.D. Carvalho, M.E. Melo Jorge, A. Gomes, M.I. da Silva Pereira, ISE NICE S04-P-110, 61st Meeting of ISE, 26 September to 1 October 2010, Nice, France, 2010
20. J. Douch, M. Hamdani, M.I. da Silva Pereira, *Port. Electrochim. Acta* 20 (2002) 3-11.